Carbohydrate Polymers 2 (1982) 171–191

CONFIGURATIONAL STATISTICS OF SINGLE CHAINS OF α-LINKED GLUCANS

DIDIER GAGNAIRE, SERGE PÉREZ‡

Centre de Recherches sur les Macromolécules Végétales (CNRS), 53X, 38041 Grenoble Cédex, France*

&

VINH TRAN†

Laboratoires de Chimie, Groupe Macromolécules Végétales, Département de Recherche Fondamentale, Centre d'Etudes Nucléaires, 85X, 38041 Grenoble Cédex, France

(Received: 23 March, 1982)

ABSTRACT

Unperturbed chain conformations are evaluated assuming separable chain configuration energies. Spatial chain propagations are constructed assuming an equiprobable occurrence of conformational states within topographically selected portions of the allowed energy space. Random coil dimensions, along with spatial representations of some single chains of α-linked glucans, such as amylose, pseudo-nigerose, nigeran and linear dextran are reported. Significant architectural differences are observed for these different α-linked glucan chains, since disordered random-coil as well as persistent pseudo-helical character, either cyclic or linear, are found, depending on the type of glycosidic linkage.

1. INTRODUCTION

Polysaccharides offer an almost unlimited range of possible structures. To understand their properties it is not only necessary to elucidate their chemical structure but also to characterise their conformations and complete three-dimensional structures. The use of accurate molecular descriptions, as drawn from the crystallographic studies on

* Laboratoire Propre du CNRS, associé à l'Université Scientifique et Médicale de Grenoble.
† Present address: Laboratoire de Stockage et de Conservation des Denrées Alimentaires, INRA, Centre de Recherches de Nantes, Chemin de la Géraudière, 44072 Nantes Cédex, France.
‡ To whom all correspondence should be addressed.

Carbohydrate Polymers 0144-8617/82/0002-0171/$02.75

sugars, oligosaccharides and their derivatives, along with the development of methods for predicting and solving the crystal structures of polysaccharides (Smith & Arnott, 1978; Zugenmaier & Sarko, 1976) have resulted in the characterisation of the three-dimensional arrangement of some polysaccharide chains. The structures of polysaccharides known so far have been shown to follow the classification proposed by Rees & Scott (1971) on the basis of a simplified form of conformational analysis.

In an effort to predict the solution properties of polysaccharides from their structure, as suggested by Brant & Dimpfl (1970), Whittington (1971) and Whittington & Glover (1972) have extended the work of Rees & Scott (1971) to a consideration of the influence of linkage geometry on the unperturbed dimensions of the chains. The characteristic ratio C_∞ was calculated from the statistical mechanical theory of polymer chain configuration (Flory, 1969, 1974). Correlations between the magnitude of C_∞ and the type of polysaccharide chains were found.

Other reports on the unperturbed dimensions of polysaccharides have appeared in the literature. Homopolymers particularly have attracted attention (Rao *et al.*, 1969; Yathindra & Rao, 1970, 1971*a*; Cleland, 1971) and in addition the sensitivity of C_∞ to the overall composition and sequence statistics of certain copolysaccharides has been investigated by Hallman & Whittington (1973). More recently, Monte Carlo techniques have been applied to amylose chains (Jordan *et al.*, 1978), pullulan and related glucans (Brant & Burton, 1981) and uronic acid polysaccharides (Bailey *et al.*, 1977).

This paper describes an alternative method for the molecular modelling of single polysaccharide chains, that can be used for complex structures as well as homopolymers. The proposed method is applied to α-linked glucans; unperturbed chain dimensions, along with three-dimensional representations, are calculated and the influence of the nature of the glycosidic linkage is investigated, with particular reference to nigeran which is a regular copolysaccharide made up of alternating $\alpha(1 \rightarrow 3)$ and $\alpha(1 \rightarrow 4)$ linkages.

2. METHODS

2.1. *Introduction*

Crystallographic investigation of oligosaccharide structures, and the extension of such studies to the elucidation of the solid state structures of polysaccharides, have led to the conclusion that separation of the polymeric backbone into rigid entities (bond lengths, bond angles and sugar ring conformations) alternately oriented about flexible linkages (the glycosidic torsion angles: Φ, Ψ, ω) is valid. It has also been shown that the allowed conformations of the poly- or disaccharide can be adequately described in terms of energy maps in (Φ, Ψ, ω) space. Because of the spatial separation afforded by the rigid sugar residues which are interpolated between the flexible linkages, the independence of the sets of glycosidic torsional angles from neighbouring sets within the polysaccharide chain has been shown to be a valid assumption, at least as a first

approximation, for almost all glycosidic linkage types except (1 → 2) linked chains. In consequence, the configurational energy for the macromolecular chains can be decomposed into additive contributions from the conformational energy of adequately chosen segments such as dimeric fragments. Spatial representative polysaccharide chains can be described by specifying values for all torsion angles (Φ_i, Ψ_i, ω_i) of the set (Brant & Gobel, 1975). Assuming that interactions between sugar residues further away than the first neighbours are not significant, a chain sample may be generated by confining examination to the conformational energy space $V(\Phi, \Psi, \omega)$ of any single independent or representative dimeric residue.

Using Monte Carlo methods, a procedure for generating and analysing chain samples has been devised by Jordan *et al.* (1978) and Brant & Burton (1981). The conformational space of a given residue is divided into an arbitrary number of rotational isomeric states equally spaced in each dimension and characterised by specific mean coordinates; each state is assigned a normalised probability, consistent with the Boltzmann factor. Under these conditions a Monte Carlo sample chain of p residues is produced and submitted to statistical analysis and graphical representation. Since in the generation, no effort is made to eliminate long-range excluded-volume interactions, and since each set of torsion angles is assumed to occur independently of all the rest, a chain of p residues can be considered as consisting of $p - x + 1$ independent chains of degree of polymerisation (DP), x, for which the properties may also be evaluated. This Monte Carlo approach depends on a knowledge of the conformational energies and therefore the reliability of the energy calculations must be considered.

In the case of α(1 → 4) linked D-glucose residues, the maltose dimer conformational states have been evaluated as a function of the glycosidic torsion angles Φ and Ψ (see following sections). A perspective plot of the three-dimensional representation of the mirror-image of the energy map is shown in Fig. 1, which clearly indicates how the concept of a *conformational energy-well* can be applied to the overall description of the low energy region encompassing the most stable states of the disaccharide. Figure 2 is the usual contour plot which is used to display the iso-energy contours as a function of the Φ and Ψ angles. Also shown in Fig. 2 are the results of a number of single crystal studies on linear and cyclic oligosaccharides containing α(1 → 4) linked D-glucose residues. The observed combinations of Φ and Ψ lie within the 4 kcal mol^{-1} contour, but are spread over a considerable portion of the energy map, and the conformations corresponding to the calculated minima are scarce. Obviously such a dispersion is a reflection on the differences occurring between linear and cyclic oligosaccharides, as well as the diversity of intermolecular environments and intermolecular packing constraints. But it clearly shows the validity of the calculated external energy contours.

On the other hand, comparison of the results obtained with different methods of calculation have shown that the *location* of the energy minima on the (Φ, Ψ) map is almost *independent* of the chosen potential energy functions, whereas the energy *differences* are *strongly dependent* on this choice (Melberg & Rasmussen, 1980). The dependence is particularly marked in the low energy regions. This suggests that energy

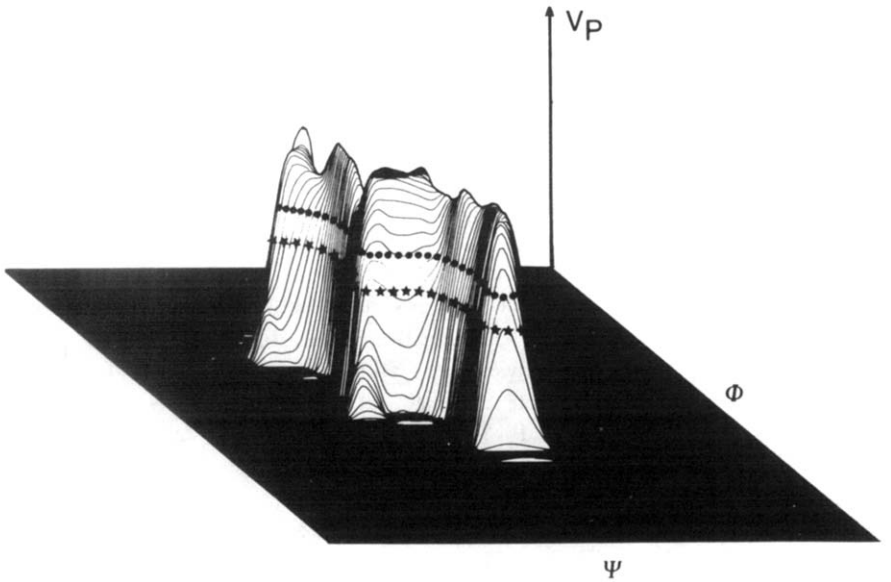

Fig. 1. Perspective drawing of the three-dimensional shape of the mirror-image of the *conformational energy well* of maltose (Mallet, 1976) for the full angular range for Φ and Ψ. The volume was constructed using the following scheme:

$$V(\Phi, \Psi) > 15 \text{ kcal mol}^{-1} \qquad V_P(\Phi, \Psi) = 0$$

$$V(\Phi, \Psi) < 15 \text{ kcal mol}^{-1} \qquad V_P(\Phi, \Psi) = -(V(\Phi, \Psi) - 15)$$

Proceeding from top to bottom of the three-dimensional shape we note: the very low energy region (shown in black); the 6 kcal mol^{-1} energy contour indicated by the dotted line; the 8 kcal mol^{-1} energy contour indicated by the line of stars.

The geometry used for the maltose unit was that determined from a neutron diffraction study (Gress & Jeffrey, 1977). The valence angle at the glycosidic oxygen atom C(1) – O(1) – C(4′) was kept at 117·5°. The potential energy was computed by taking into account the van der Waals, torsional and hydrogen-bond contributions. A three-fold intrinsic torsional potential was used for rotations about Φ (H(1) – C(1) – O(1) – C(4′)) and Ψ (H(4′) – C(4′) – O(1) – C(1)) with barriers 0·9 and 2·7 kcal mol^{-1}, respectively. The conformational energy $V(\Phi, \Psi)$ was computed for the full angular range for Φ and Ψ over a 5° interval.

surfaces are valuable in defining the pertinent portion of the map embodying 'allowed' conformations but absolute energy values should be treated with caution.

For this reason instead of a Monte Carlo approach where the probability assigned to each angle pair (Φ, Ψ) is weighted by a Boltzmann function according to the dimer energy, an alternative Monte Carlo type of approach is proposed based on the equiprobable occurrence of conformational states within a portion of the energy surface.

2.2. *Generation and Analysis of Chain Samples*

Conformational energy surfaces $V(\Phi, \Psi)$ were evaluated using methods described previously (Tvaroska *et al.*, 1978) for the full angular range, varying the glycosidic

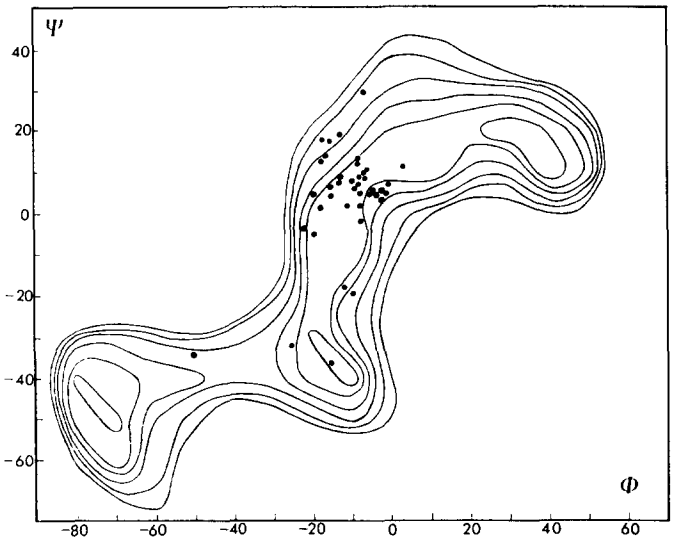

Fig. 2. Energy diagram computed in terms of Φ and Ψ for two (1 → 4)-α-linked glucose residues (Pérez *et al.*, 1979), where Φ = (H(1) – C(1) – O(1) – C(4′)) and Ψ = (H(4′) – C(4′) – O(1) – C(1)). Contours are given at intervals of 1 kcal mol^{-1} and are expressed relative to the minimum. •, Denotes an observed combination of (Φ, Ψ) as found in crystal structures of linear and cyclic oligosaccharides with glucose residues. This figure is an updated presentation of a previously published figure (Pérez *et al.*, 1979) where the pertinent references were listed. The solid state conformations (Φ = −3·6, Ψ = 4·1) as found for α-maltose (Takusagawa & Jacobson, 1978) and (Φ = −25, Ψ = −34) as found for β-maltose octa-acetate (Brisse, F., Marchessault, R. H., Pérez, S. & Zugenmaier, P., to be published) have been added to the present version.

torsion angles over a given interval (typically 5°). Provision was made to include the influence of pendant groups on the resulting $V(\Phi, \Psi)$ maps. The three-dimensional representation of the total energy map, shown in Fig. 1, brings out the features of the energy map more clearly and is also suited for extracting quantitative information such as the magnitude of the energy value which is going to determine the cut-off limit associated with the energy well. Two other methods were also used to determine this cut-off limit. Firstly, the computation of the energy surface delineated by the maximum of the first derivative of the energy surface with respect to the angles Φ and Ψ. The CARTOLAB system (Mallet, 1976) used to produce the conformational energy well shown in Fig. 1, also allows the computation of contours of the gradient with respect to the surface. The cut-off energy is the minimum value of the energy contour which completely encloses the region defined by the maximum gradient. Secondly, a somewhat simpler method can be employed by evaluating the surfaces $S(E_K)$ embodied by successive iso-energy contours (E_K); the cut-off limit being reached when the ratio $S(E_K - 1)/S(E_K)$ is less than a given value (typically 0·05).

The three-proposed methods of calculation all yield essentially the same result. For computational purposes the external limit contour is approximated to a polygon. All

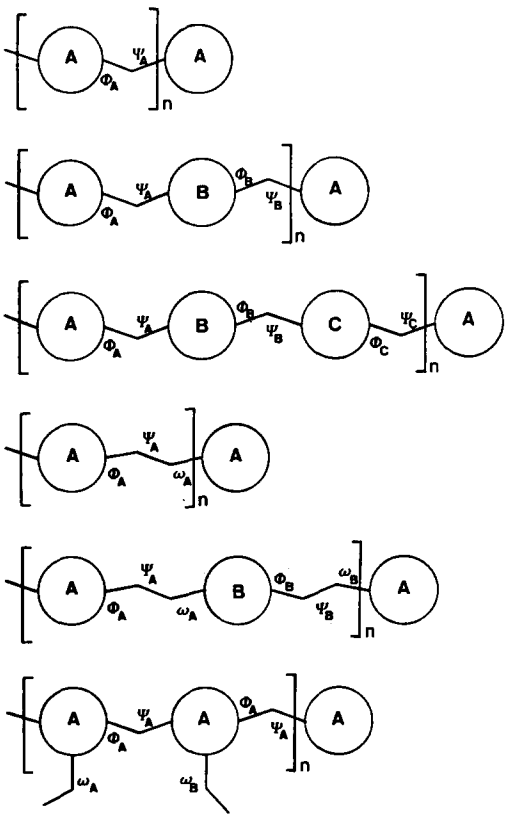

Fig. 3. Types of polymeric structure that can be investigated using the method described with the associated set of computer programs. A, B, C denote sugar rings (or any rigid entity), the variable parameters being Φ_i, Ψ_i and ω_i.

conformational states belonging to the pertinent domain are given an equiprobable occurrence. By utilising a pseudo-random numbers generator, $p - 1$ angle pairs $(\Phi, \Psi)_i$ are generated. Since the monomeric residue is approximated to a rigid backbone with only two variable torsion angles (Φ and Ψ), a sequence of p residues can be constructed; the coordinates of the glycosidic oxygen atoms (or of any atom of interest) are stored. Therefore investigation of any conformational properties of interest along with graphical representations can be performed.

Because of the intrinsic simplicity arising from the assumption of an equiprobable occurrence of (Φ, Ψ) angles, within a defined domain, the generation of quite complex polysaccharide chain samples is possible. Figure 3 summarises the type of polymeric structures that can be investigated using this procedure. Extension to more complicated cases is easy, provided the extra computer core is available.

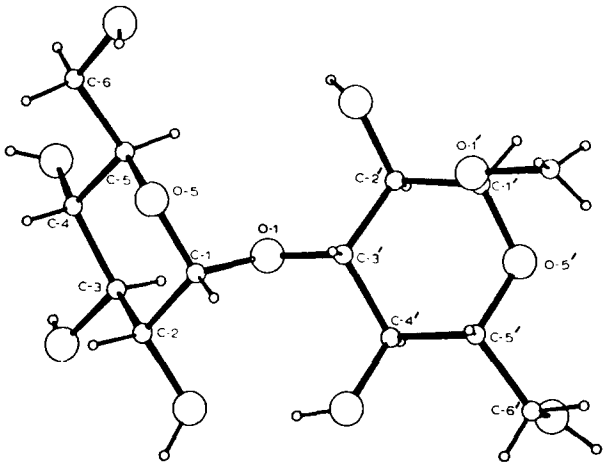

Fig. 4. View of the molecule of nigerose as found in the solid state (Neuman *et al.*, 1980). Torsion angles ϕ and ψ denote rotation about the glycosidic bond C(1) – O(1) and O(1) – C(3′). $\phi = |H(1) - C(1) - O(1) - C(3')|$ and $\psi = |H(3') - C(3') - O(1) - C(1)|$. The magnitude of the glycosidic valence angle C(1) – O(1) – C(3′) is 116·2°.

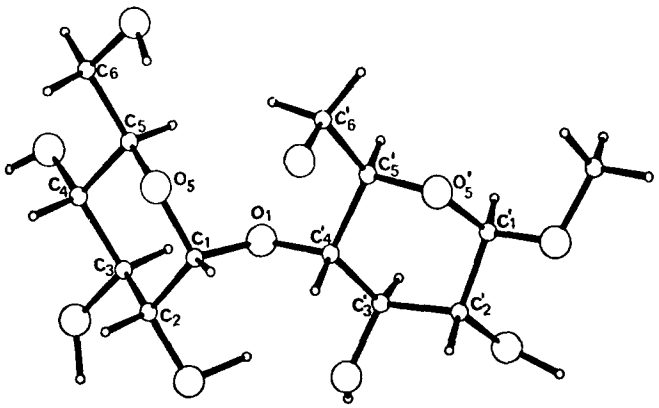

Fig. 5. View of the molecule of β-maltose as found in the solid state (Gress & Jeffrey, 1977). Torsion angles ϕ and ψ denote rotation about the glycosidic bond C(1) – O(1) and O(1) – C(4′); $\phi = |H(1) - C(1) - O(1) - C(4')|$ and $\psi = |H(4') - C(4') - O(1) - C(1)|$. The magnitude of the glycosidic valence angle C(1) – O(1) – C(4′) is 117·5°.

Estimation of the unperturbed polymers chain dimensions such as the characteristic ratio $C_x = \langle r^2 \rangle_0 / xL^2$, is carried out using the method of Jordan *et al.* (1978). For this purpose the polysaccharide chain is treated as a set of x virtual bonds (L) linking the glycosidic oxygen atoms, $\langle r^2 \rangle_0$ being the mean squares end-to-end length over all conformations. Similarly, the magnitude of the mean end-to-end vector, denoted as 'persistence length' can be evaluated.

Pictures of specific chains chosen as representative of several surveyed, can be readily obtained from the sets of stored atomic coordinates. For this purpose, the circles represent the glycosidic oxygen atoms, which are shown connected in sequence by virtual bonds (the sugar residues have been omitted). It should be pointed out that these drawings represent a conformation of a chain sample at a given instant.

All the calculations were performed on a Honeywell-Bull CII 'HB-68' computer at the Université de Grenoble, using a set of programs specially designed for this work.

2.3. *Polysaccharide Structures Studied*

For the present investigation four different α-D-glucans have been selected: pseudo-nigeran ($(\alpha(1\rightarrow 3)-\mathrm{Glc})_n$), amylose ($(\alpha(1\rightarrow 4)-\mathrm{Glc})_n$), dextran ($(\alpha(1\rightarrow 6)-\mathrm{Glc})_n$) and the nigeran polydisaccharide ($(\alpha(1\rightarrow 4)-\mathrm{Glc}-\alpha(1\rightarrow 3)-\mathrm{Glc})_n$). The $\alpha(1\rightarrow 2)$ linked glucans have not been considered since independence of the sets of glycosidic torsion angles from neighbouring sets cannot be justified. Figures 4, 5, 6 and 7 show the relevant structures while the geometric information required for the calculations is summarised in Table 1.

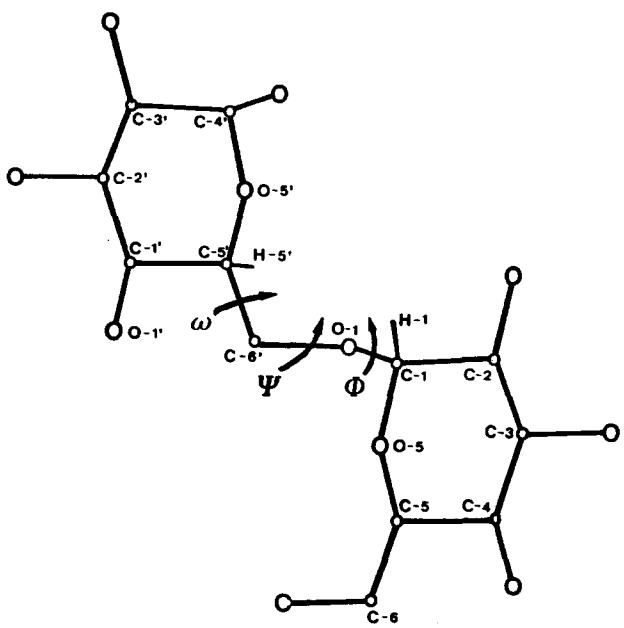

Fig. 6. View of the repeating disaccharide unit of dextran as deduced from conformational analysis (Tvaroska *et al.*, 1978). Torsion angles ϕ, ψ and ω denote rotation about the glycosidic bond C(1) – O(1), O(1) – C(6′) and C(6′) – C(5′), respectively. $\phi = |\mathrm{H(1)-C(1)-O(1)-C(6')}|$; $\psi = |\mathrm{C(1)-O(1)-C(6')-C(5')}|$ and $\omega = |\mathrm{O(1)-C(6')-C(5')-O(5')}|$. The magnitude of the glycosidic valence angle C(1) – O(1) – C(6′) is 111·5°.

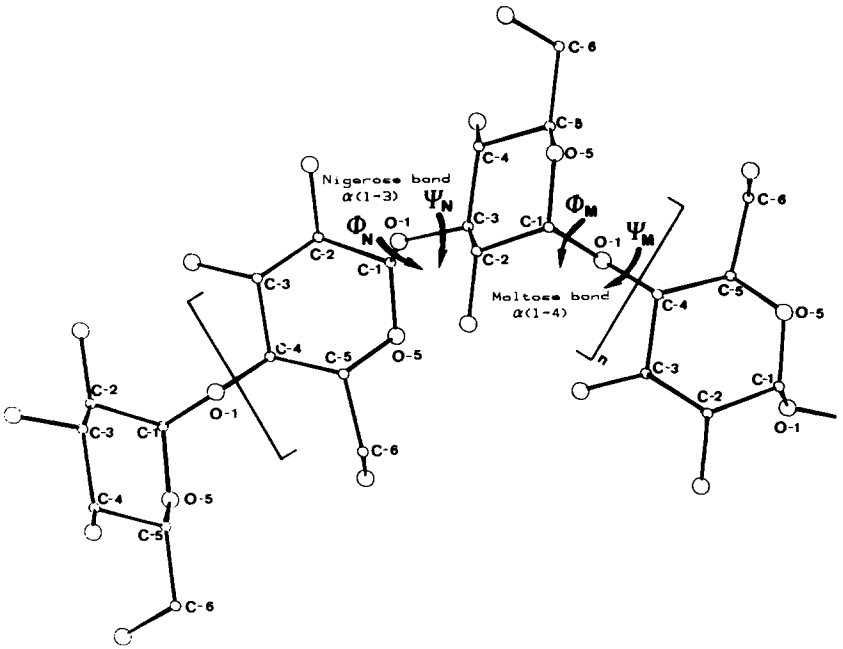

Fig. 7. View of the repeating tetrasaccharide unit as found in nigeran from structural studies based on electron and X-ray diffraction analysis (Pérez *et al.*, 1979). Torsion angles ϕ_M, ψ_M and ϕ_N, ψ_N denote rotations about the glycosidic bonds of the maltose ($\alpha(1\rightarrow4)$) and nigerose ($\alpha(1\rightarrow3)$) linkage, respectively. $\phi_M = |H(1)-C(1)-O(1)-C(4')|$; $\psi_M = |H(4')-C(4')-O(1)-C(11)|$; $\phi_N = |H(1)-C(1)-O(1)-C(3')|$ and $\psi_N = |H(3')-C(3')-O(1)-C(11)|$. The magnitude of the glycosidic valence angle C(1) – O(1) – C(3′) = 116·2° and C(1) – O(1) – C(4′) = 117·5°.

3. RESULTS AND DISCUSSION

3.1. *The Amylose Chain Configuration* ($\alpha(1\rightarrow4-\mathrm{Glc})_n$)

The maltose dimer conformational energy surface was taken from previous work (Pérez *et al.*, 1979) and the crystal structure data was derived from the neutron study on β-maltose monohydrate (Gress & Jeffrey, 1977). It was shown that the relative orientations of the primary hydroxyl groups (Pérez *et al.*, 1979) had no significant effect on the overall features of the $V(\Phi,\Psi)$ energy surface. Topographical analysis of the iso-energy contours indicates that 6 kcal mol^{-1} above the absolute energy minimum was a reasonable value to define the domain of occurrence of equiprobable conformations, the area of surface of the domain being $4760^{\circ 2}$ (Fig. 8). The contour region spans the domains of residue conformations possessing both left- and right-handed helical chirality.

In order to test the validity of the proposed approach, as compared to the method used by Jordan *et al.* (1978) and Brant & Barton (1981), the case of amylose was

TABLE 1
Geometrical Information Used in the Generation of the Four Polysaccharides

Polysaccharide	*Geometrical parameters*	L (Å) *virtual bond*	P, *Number of residues in the chain samples*
$((\alpha(1\rightarrow 3)-\mathrm{Glc})_n)$	$(-O(1)-C(3)-C(2)-C(1)-)-O(1)$		
	$C(1)-O(1)=1{\cdot}405$ Å $C(2)-C(1)-O(1)=107{\cdot}4°$ $C(3)-C(2)-C(1)-O(1)=-63{\cdot}3°$	4·28	2 000
	$O(1)-C(3)=1{\cdot}433$ Å $C(1)-O(1)-C(3)=116{\cdot}2°$ $C(2)-C(1)-O(1)-C(3)=\Phi^{C(2)a}$		
	$C(3)-C(2)=1{\cdot}523$ Å $O(1)-C(3)-C(2)=108{\cdot}5°$ $C(1)-O(1)-C(3)-C(2)=\Psi^{C(2)a}$		
	$C(2)-C(1)=1{\cdot}528$ Å $C(3)-C(2)-C(1)=109{\cdot}9°$ $O(1)-C(3)-C(2)-C(1)=-173{\cdot}4°$		
$((\alpha(1\rightarrow 4)-\mathrm{Glc})_n)$	$(-O(1)-C(4)-C(3)-C(2)-C(1)-)-O(1)$		
	$C(1)-O(1)=1{\cdot}413$ Å $C(2)-C(1)-O(1)=108{\cdot}6°$ $C(3)-C(2)-C(1)-O(1)=-64{\cdot}3°$	4·39	2 000
	$O(1)-C(4)=1{\cdot}420$ Å $C(1)-O(1)-C(4)=117{\cdot}5°$ $C(2)-C(1)-O(1)-C(4)=\Phi^{C(2)a}$		
	$C(4)-C(3)=1{\cdot}526$ Å $O(1)-C(4)-C(3)=108{\cdot}0°$ $C(1)-O(1)-C(4)-C(3)=\Psi^{C(3)a}$		
	$C(3)-C(2)=1{\cdot}528$ Å $C(4)-C(3)-C(2)=110{\cdot}1°$ $O(1)-C(4)-C(3)-C(2)=174{\cdot}6°$		
	$C(2)-C(1)=1{\cdot}531$ Å $C(3)-C(2)-C(1)=110{\cdot}9°$ $C(4)-C(3)-C(2)-C(1)=-51{\cdot}4°$		
$((\alpha(1\rightarrow 6)-\mathrm{Glc})_n)$	$(-O(1)-C(6)-C(5)-C(1)-)-O(1)$		
	$C(1)-O(1)=1{\cdot}406$ Å $O(5)-C(1)-O(1)=111{\cdot}4°$ $C(5)-O(5)-C(1)-O(1)=59{\cdot}5°$	4·77	2 000
	$O(1)-C(6)=1{\cdot}433$ Å $C(1)-O(1)-C(6)=112{\cdot}0°$ $O(5)-C(1)-O(1)-C(6)=\Phi^{O(5)a}$		
	$C(6)-C(5)=1{\cdot}502$ Å $O(1)-C(6)-C(5)=109{\cdot}5°$ $C(1)-O(1)-C(6)-C(5)=\Psi^{C(5)a}$		
	$C(5)-O(5)=1{\cdot}439$ Å $C(6)-C(5)-O(5)=109{\cdot}0°$ $O(1)-C(6)-C(5)-O(5)=\omega^{O(5)a}$		
	$O(5)-C(1)=1{\cdot}419$ Å $C(5)-O(5)-C(1)=113{\cdot}4°$ $C(6)-C(5)-O(5)-C(1)=-175{\cdot}0°$		
$((\alpha(1\rightarrow 3)-\mathrm{Glc}-\alpha(1\rightarrow 4)-\mathrm{Glc})_n)$	$(-O(1)-C(3)-C(2)-C(1)-O(1')-C(4')-C(3')-C(2')-C(1)-)-O(1)$		2 000

[a] Appropriate translations of ± 120° must be applied to the Φ and Ψ torsional angles for conversion to the angle referred to an hydrogen atom.

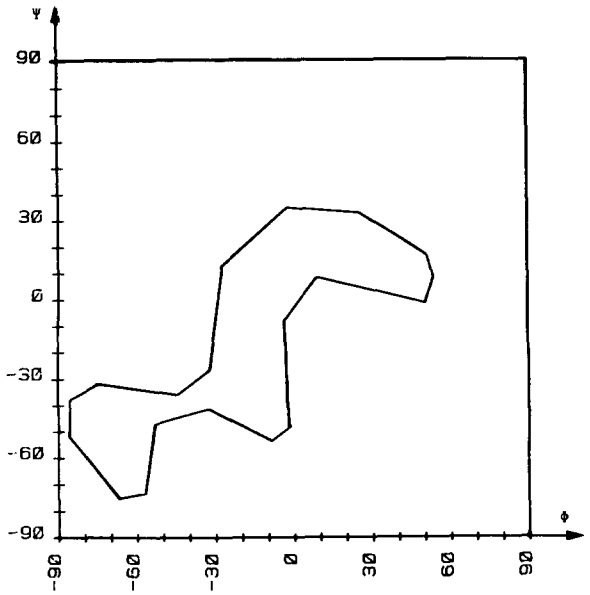

Fig. 8. Domain of occurrence of equiprobable conformations for rotations about ϕ and ψ underlying the propagation of amylose chains.

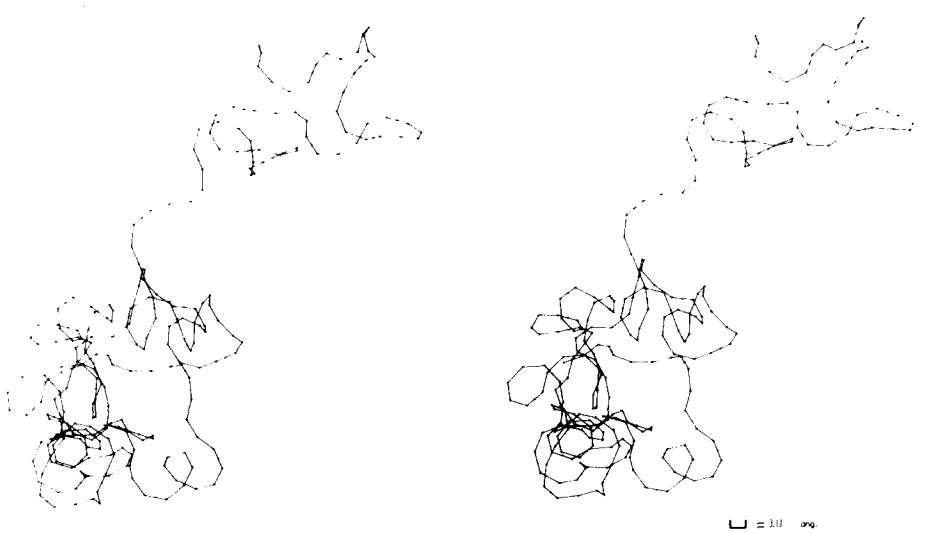

Fig. 9. Stereoscopic view of a representative 250 residue amylose chain consistent with the energy domain of Fig. 8. Dots represent glycosidic oxygens, lines are virtual bonds, arrows displayed every five residues indicate the propagating direction.

submitted to detailed investigation. Typically, chain samples with $p = 2000$ were generated. Figure 9 represents a diagram of a 250 residue chain, selected from among several samples studied. As previously observed (Jordan *et al.*, 1978), the amylose chain displays a pseudo-helical tendency with the occurrence of cycloamylose-like loops. The dependence of C_x on x for amylose chain samples is shown in Fig. 10. It can be seen that a value of 2 for C_∞ is suggested. The presence of local minima in the plot of C_x against x for small values of x is further evidence of the tendency for helix formation. This can also be seen from Fig. 11 which displays the probability $P_x(R)$ that terminal segments of a chain of x segments will approach within the distance R. For the present study, values of R (R being the distance between the glycosidic oxygen atom of residue i and glycosidic oxygen atom of residue $i + x$) in the range 1-7 Å, was selected. Values less than 4-5 Å, correspond to spatial arrangements where self-intersection is highly probable. Figure 11 shows that maxima in the functions $P_x(R)$ occur at $x \simeq 8$-9, $x \simeq 16$, $x \simeq 24$, $x \simeq 32$; this is in agreement with the helical loop formations disclosed in Fig. 10. Figure 11 does reveal an inadequacy in the present model, since it shows that chain segments are allowed to approach to within sterically impossible positions ($R < 5$ Å). This would tend to indicate that the occurrence of helical formations as observed in the present chain model is overestimated, but nevertheless it is apparent from the data in Fig. 11 for $R > 5$ Å that it is an intrinsic characteristic of the architecture of the amylose chain.

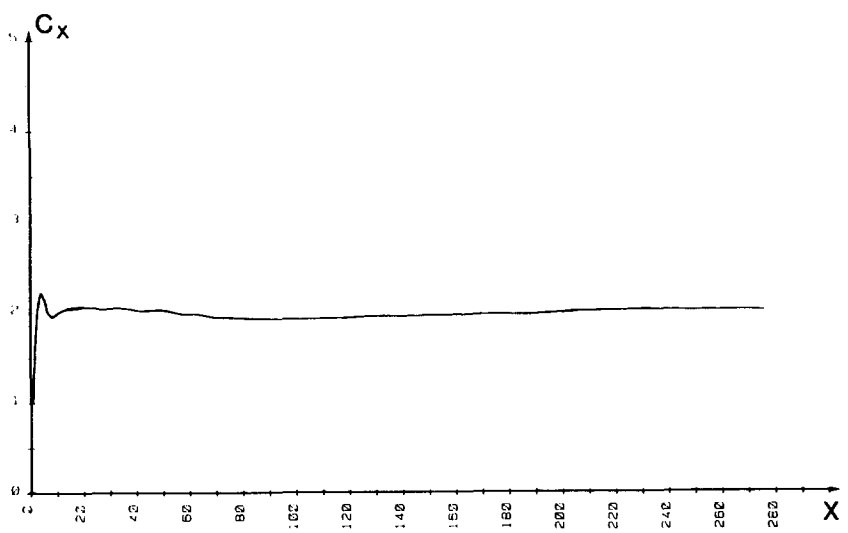

Fig. 10. Characteristic ratio C_x as a function of chain length x, from a sample of 2000 chains.

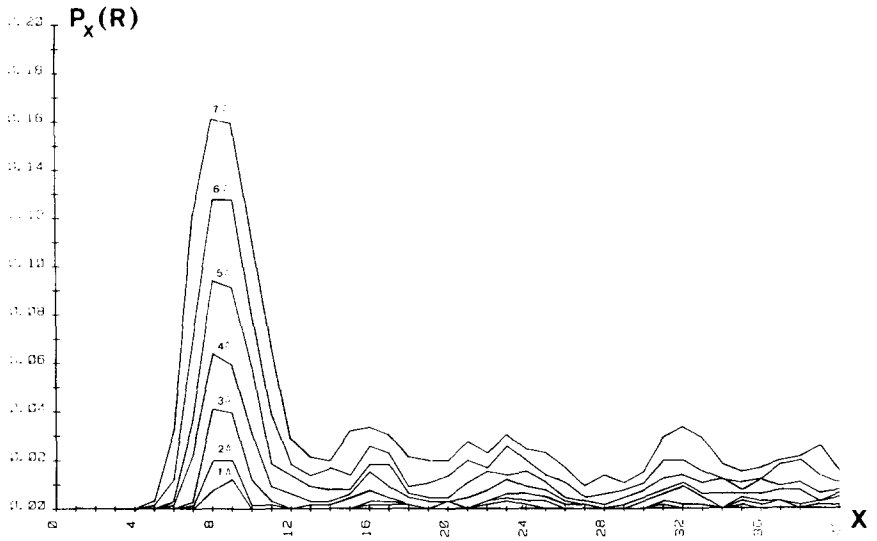

Fig. 11. The probability $P_x(R)$ that terminal segments within a chain of x segments will approach within the distance R plotted as a function of x for R = 1-7 Å.

3.2. *The Pseudo-Nigeran Chain Configuration* $((\alpha(1 \rightarrow 3) - \mathrm{Glc})_n)$

The pseudo-nigeran dimer conformational energy surface was calculated from the crystal structure data of Neuman *et al.* (1980). The $V(\Phi, \Psi)$ energy surface was shown to be independent of the relative orientations of the primary hydroxyl groups. Here again the 6 kcal mol^{-1} energy value above the absolute minimum was selected to define the domain of occurrence of equiprobable conformations, area of the surface of this domain being about $8390°^2$ (Fig. 12). Figure 13 depicts a projection drawing of a particular pseudo-nigeran chain conformation consistent with the preceding domain. The chain is considerably extended and displays portions where a pseudo-helical 2_1 propagation can be visualised. Nevertheless some folds are shown to occur. The study of the variations of C_x on x indicates C_x is independent of x for $x > 800$ suggesting an extended chain with a value of C_∞ of about 30.

3.3. *The Dextran Chain Configuration* $(\alpha(1 \rightarrow 6) - \mathrm{Glc})_n$

The relative orientation of two contiguous residues is described by three torsional angles Φ, Ψ and ω as shown in Fig. 6. A previous conformational energy investigation (Tvaroska *et al.*, 1978) has shown that the three-dimensional energy space is a 'cylinder' with an irregular cross-section. The cylinder is extended parallel to the ω axis, the allowed conformational space being restricted to an area around $\omega = 180°$, $\omega = 60°$ and $\omega = -60°$. Therefore the dextran chain may be created by restricting consideration to the three conformational energy surfaces: $V(\Phi, \Psi, \omega = 60°)$, $V(\Phi, \Psi, \omega = -60°)$

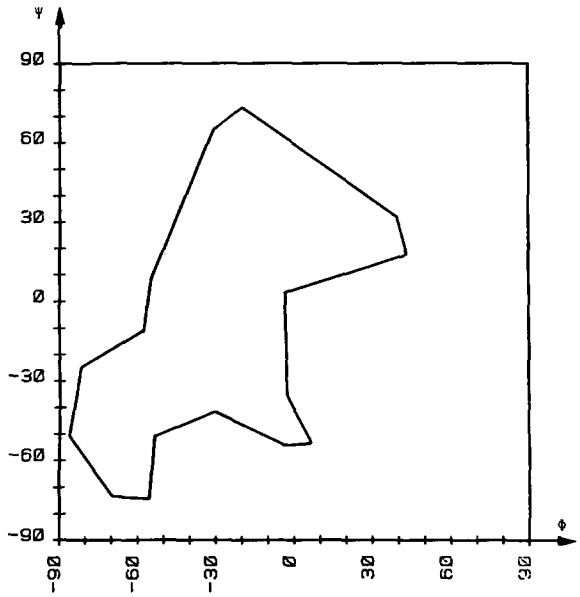

Fig. 12. Domain of occurrence of equiprobable conformations for rotations about Φ and Ψ underlying the propagation of pseudo-nigeran chains.

and $V(\Phi, \Psi, \omega = 180°)$. One important parameter is the relative occurrence of these preferred conformations about the ω angle. A survey of the conformations of the hydroxymethyl groups (rotations about ω) in crystalline aldohexopyranoses (Marchessault & Pérez, 1979) has indicated that for a *gluco* configuration, the conformers corresponding to values of $\omega = -60°$ and $\omega = 180°$ occur in ratios of 60% and 40%, respectively. In order to account for the non-occurrence of the third conformer ($\omega = 60°$) in small molecules in the solid state, stereoelectronic effects may be invoked with an energy of about 3 kcal mol^{-1} associated with this effect (Marchessault & Pérez, 1979). Hence this energy has to be added to the energy surface $V(\Phi, \Psi, \omega = 60°)$. The portions of the three energy surfaces corresponding to conformations no greater than 6 kcal mol^{-1}, above the lowest energy minimum, are shown in Fig. 14. The dextran chain conformation as depicted in Fig. 15 was generated assuming the occurrence of a given energy section as a function of ω was proportional to its relative surface area ($17\,700°^2(\omega = 180°)$; $11\,910°^2(\omega = -60°)$ and $6230°^2(\omega = 60°)$. The variation of C_x with x showed that C_x was independent of x for $x > 150$, yielding a value of 4·7 for C_∞.

3.4. *The Nigeran Chain Configuration* ($(\alpha(1 \rightarrow 4)$ Glc $- \alpha(1 \rightarrow 3)$ Glc$)_n$)

The glucan nigeran is a copolysaccharide of D-glucopyranose residues alternately linked $\alpha(1 \rightarrow 3)$ and $\alpha(1 \rightarrow 4)$. The chemical repeating sequence is either a maltose

Fig. 13. Perspective drawing of a representative 250 residue pseudo-nigeran chain, consistent with the energy domain of Fig. 12.

with rotation angles (Φ_N, Ψ_N) or a nigerose with rotation angles (Φ_M, Ψ_M). The nigeran conformation depicted in Fig. 15 was generated using the energy surface of Fig. 8 for the $\alpha(1 \rightarrow 4)$ linkage and the surface of Fig. 12 for the $\alpha(1 \rightarrow 3)$ linkage. For the nigeran C_x was independent of x for $x > 600$ and C_∞ was evaluated as 13. Thus the effect of introducing into the amylose backbone periodic $\alpha(1 \rightarrow 3)$ linkages is to give a somewhat extended chain as shown on the projection drawing (Fig. 16).

3.5. *Comparison with other Monte Carlo Studies of Polysaccharide Chains*

For amylose the results from this study are in qualitative agreement with other Monte Carlo studies. The graphical representation of the amylose chain, along with the value for the probability $P_x(R)$ that terminal segments of a chain of x segments will approach within a given distance, are similar to those reported previously (Jordan *et al.*, 1978). Also, the values obtained for C_∞ are of the same order of magnitude

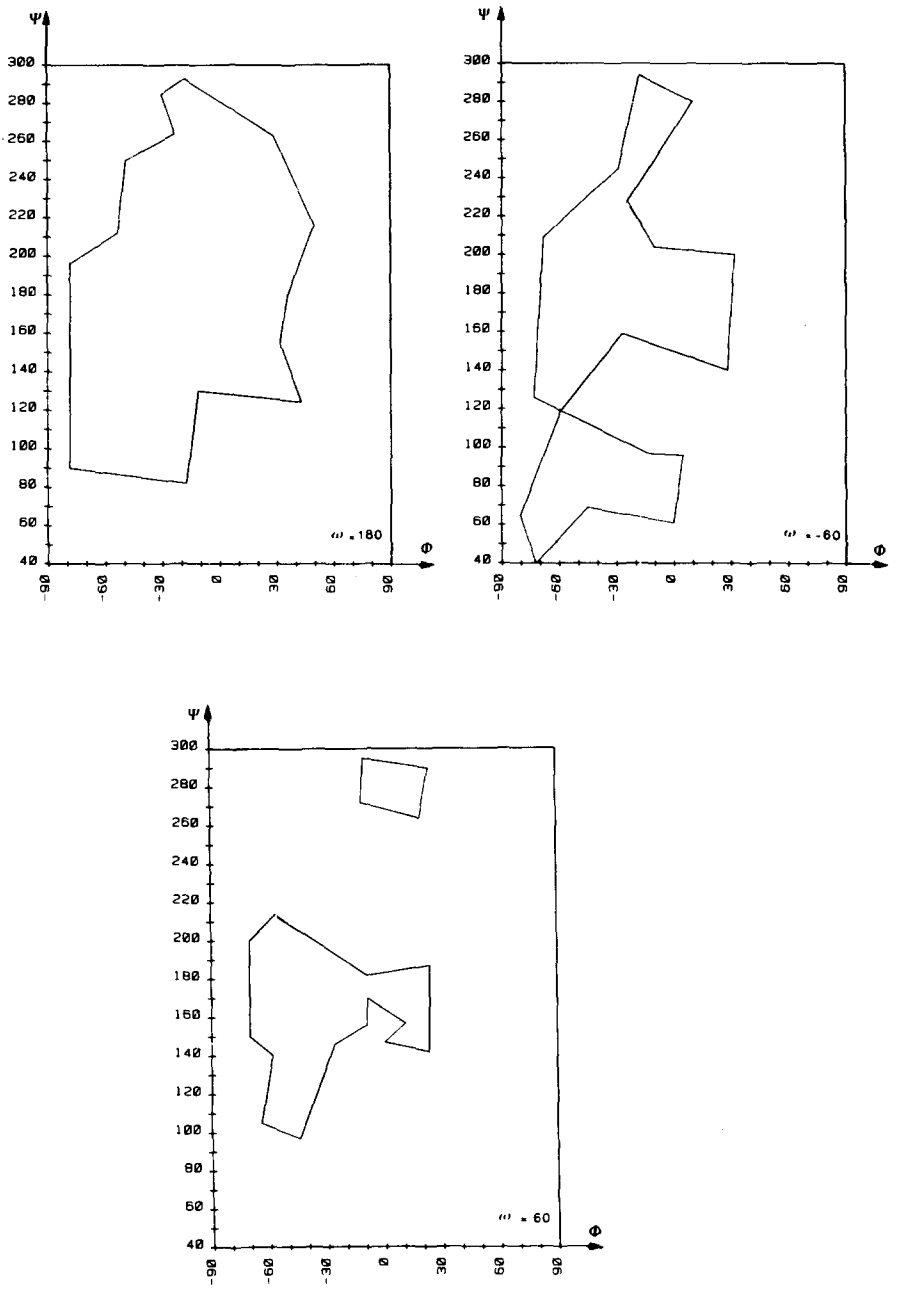

Fig. 14. Domains of occurrence of equiprobable conformations for rotations about ϕ, ψ and ω underlying the propagation of dextran chains.

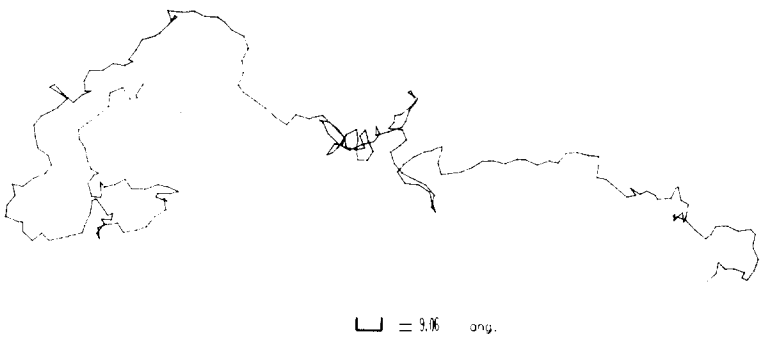

Fig. 15. Perspective drawing of representative 250 residue dextran chains, consistent with the energy domains of Fig. 14.

Fig. 16. Perspective drawing of representative 250 residue nigeran chains, consistent with the energy domains of Fig. 5 and Fig. 12, respectively.

(4 and 2, respectively). It should be noticed that the value of the characteristic ratio is very much dependent on geometrical parameters such as the magnitude of the glycosidic bridge angle (Brant & Goebel, 1975). In both studies plots of C_x against x show that C_x is constant for DP values greater than about 200. A detailed explanation of the observed differences will be reported elsewhere (Tran, 1982). General agreement is obtained despite the fact that different methods as well as different energy surface were used.

For the dextran case, recent investigations (Brant & Burton, 1981) based on a Monte Carlo approach, yield values for C_∞ that vary from 1·8 to 5, depending on the nature of the potential functions used. Here again, our calculated value of 4·7 is of the same order of magnitude. Table 2 summarises the different values reported for C_∞ for α-linked glucan chains, according to different methods of calculation.

TABLE 2
Comparison of Characteristic Ratios of α-Glucan Chains According to Different Methods of Calculations

	C_x	C'_x[a]	*Reference*
α(1 → 3)	37	1·47	Whittington *et al.* (1972)
	30		Present work
α(1 → 4)	4·4	1·14	Jordan *et al.* (1978)
	4·6		Whittington *et al.* (1972)
	6·8		Rao *et al.* (1969)
	2·0		Present work
α(1 → 6)	1·8		Brant *et al.* (1981)
	4·7		Present work

[a] Characteristic ratio of freely rotating chains (valence angle = 117·5°), Yathindra & Rao (1971*b*).

3.6. *The Architectural Differences*

For all cases studied, it is found that the chains have a statistical or random coil conformation. However, significant differences between polysaccharides are found both in terms of the magnitude of the characteristic ratios and the pictures of representative chains. Dextrans show the most 'disordered' conformation with abrupt changes in direction and an apparent lack of pseudo-helical tendency. A helical tendency is found in the case of the α(1 → 4) and α(1 → 3) glucans. For the homoglucans there does exist a correlation between the calculated unperturbed dimensions, the spatial representations and the classification suggested by Rees & Scott (1971). The α(1 → 3)-D-glucan chain has the highest value of the characteristic ratio and is extended (Type A), whereas the amylose chain possesses the lowest value of C_∞ and has loops (Type B). Although the dextran chain exhibits abrupt changes in direction it is on average extended in character (Type D). Type C is rarely encountered and should correspond to α(1 → 2) linked homoglucans.

An important feature displayed by the present work is the persistence of a pseudo-helical order in the generated α(1 → 4) and α(1 → 3) glucan chains. As noticed previously the surface encompassed by the allowed domain for the α(1 → 3) linked dimer is about 8390°², whereas the one for the α(1 → 4) dimer is about 4760°². Hence the pseudo-helical tendency cannot be associated solely with the notion of conformational freedom. Instead of using the glycosidic torsion angles and the (Φ, Ψ, ω) repre-

sentation, spatial organisation of the chains can be equally well defined by consecutive fragments having orientations characterised by values of the helical parameters (n, h) where n is the number of residues per turn of the helix and h is the translation of the corresponding residues along the helix axis. The distribution of helical parameters rather than the distribution of the conformational angles is more suitable for defining the occurrence of any helical or pseudo-helical tendency. Using an algorithm reported previously (Gagnaire *et al.*, 1980) the (n, h) values corresponding to the sets of glycosidic torsion angles (Φ, Ψ) underlying the spatial propagation, respectively, of $\alpha(1 \rightarrow 3)$ and $\alpha(1 \rightarrow 4)$ glucan chains, have been calculated. In the case of $\alpha(1 \rightarrow 4)$ linkage, the helical parameters are centred around $n = 2$ (maximum $n = \pm 3$), h having values running from 3·64 Å to the maximum elongation of 4·28 Å. In both cases, the range of n and h parameters is limited, and this explains the persistence of the pseudo-helical tendency in the diluted chains.

The comparison between the amylose and pseudo-nigeran fully illustrates the concepts of flexibility versus chain stiffness as already discussed by Brant & Goebel (1975). The conformational space available for the $\alpha(1 \rightarrow 3)$ linkage is twice as large as the one associated with rotations about the $\alpha(1 \rightarrow 4)$ glycosidic bonds. Therefore, the pseudo-nigeran should be considered in that case, as more *flexible*, in terms of conformational freedom. On the other hand, comparisons of the characteristic ratios, along with the spatial representations obtained for the $\alpha(1 \rightarrow 3)$ and $\alpha(1 \rightarrow 4)$ linkages, show that the pseudo-nigeran chain is much more extended and should be considered as *stiffer* than the amylose chain.

For nigeran, it is interesting to note how the periodic $\alpha(1 \rightarrow 3)$ linkage in the amylose backbone destroys the loop-forming tendency of the original polysaccharide. This is indicated both by the large characteristic ratio of 13 and the projection drawing (Fig. 15). The nigeran chain is extended and could be classified as belonging to the Type A structure proposed by Rees & Scott (1971). As a matter of fact, the solid state structural model found for anhydrous nigeran (Pérez *et al.*, 1979) is based on a 2_1 helix and involves a 'corrugated ribbon' type of chain. Nevertheless, the spatial representation discloses occasional folds, occurring from a combination of $\alpha(1 \rightarrow 3)$ conformations that combine with those of the $\alpha(1 \rightarrow 4)$ linkage in the segment to create short sequences with an amylose-like trajectory. In our opinion, the two-fold characteristics of the nigeran polymer, as disclosed from the present work, i.e. an extended chain along with the possibility of folding, should be connected to the fact that folding chain crystals can be grown from solution for samples having a degree of polymerisation as high as 3000.

4. CONCLUSION

The proposed method of conformational analysis is based on the assumption of an equiprobable occurrence of conformations within a selected portion of the conformational space. Because of the intrinsic simplicity arising from this assumption, the generation and statistical analysis of quite complex polysaccharide chains is feasible.

Application of this method to some simple homoglucans yields chain characterisations defined in terms of statistically averaged unperturbed dimensions and spatial representations of individual chains. Comparisons with results obtained through the application of other methods shows that general agreement is reached. This can be considered as satisfactory, specially when one is aware of the extreme dependence of the unperturbed dimensions on the value chosen for the valence angle at the bridge oxygen, as well as on the type of potential functions used. Being in a position to predict characteristic ratios quantitatively for well characterised systems, provides a way of classifying polysaccharide structures either for homo- or for heteroglucans.

Using the proposed method the influence of a number of features (bridge angle, ring conformations, pendant groups, etc.,...) on the generated chain samples can be investigated even in the case of complex heteroglucans. The process of propagating the polymer chains allows for the calculation and storage of the atomic coordinates of any group of interest. Some dynamical properties can be related to the spatial dispersion of vectors associated with atomic coordinates. Hence, the statistical study of the dispersion of these vectors should yield a comprehensive approach, at a molecular level, to the dynamical behaviour of polysaccharide chains.

ACKNOWLEDGEMENTS

We are pleased to acknowledge the collaboration of Mrs M. L. Dheu-Andries (CERMAV) and Mr E. Sibut (Centre Interuniversitaire de Calcul de Grenoble) who produced the perspective plot of the three-dimensional representation of the amylose conformational energy well using the CARTOLAB library.

REFERENCES

Bailey, E., Mitchell, J. R. & Blanshard, J. M. V. (1977). *Colloid and Polymer Sci.* **255**, 856.
Brant, D. A. & Burton, B. A. (1981). *Solution properties of polysaccharides*, ACS Symposium Series, No. 7.
Brant, D. A. & Dimpfl, W. L. (1970). *Macromolecules* **3**, 655.
Brant, D. A. & Goebel, K. D. (1975). *Macromolecules* **8**, 522.
Cleland, R. L. (1971). *Biopolymers* **10**, 1925.
Flory, P. J. (1969). *Statistical mechanics of chain molecules*, Wiley Interscience, New York.
Flory, P. J. (1974). *Macromolecules* **7**, 381.
Gagnaire, D., Pérez, S. & Tran, V. (1980). *Carbohydr. Res.* **78**, 89.
Gress, M. & Jeffrey, G. A. (1977). *Acta Crystallogr.* **B33**, 2490.
Hallman, G. M. & Whittington, S. G. (1973). *Macromolecules* **6**, 388.
Jordan, R. C., Brant, D. A. & Cesaro, A. (1978). *Biopolymers* **17**, 2617.
Mallet, J. L. (1976). *Programmes de cartographie automatique*, Présentation de la Bibliothèque CARTOLAB, Sciences de la Terre, Série 'Informatique Géologique, No. 7, Nancy, France.
Marchessault, R. H. & Pérez, S. (1979). *Biopolymers* **18**, 2369.
Melberg, S. & Rasmussen, Kj. (1980). *Carbohydr. Res.* **78**, 215.
Neuman, A., Avenel, D., Arene, F. & Gillier-Pandraud, H. (1980). *Carbohydr. Res.* **80**, 15.

Pérez, S., Roux, M., Revol, J. F. & Marchessault, R. H. (1979). *J. Mol. Biol.* **129**, 113.
Rao, V. S. R., Yathindra, N. & Sundararajan, P. R. (1969). *Biopolymers* **8**, 325.
Rees, D. A. & Scott, W. E. (1971). *J. Chem. Soc., B* 469–79.
Smith, P. J. C. & Arnott, S. (1978). *Acta Crystallogra.* **A34**, 3.
Tagusagawa, F. & Jacobson, R. A. (1978). *Acta Crystallogra.* **B34**, 213.
Tran, V. (1982). *Thèse de Doctorat*, Université Scientifique et Médicale de Grenoble, France.
Tvaroska, I., Pérez, S. & Marchessault, R. H. (1978). *Carbohydr. Res.* **61**, 97.
Whittington, S. G. (1971). *Macromolecules* **4**, 569.
Whittington, S. G. & Glover, R. M. (1972). *Macromolecules* **5**, 55.
Yathindra, N. & Rao, V. S. R. (1970). *Biopolymers* **9**, 783.
Yathindra, N. & Rao, V. S. R. (1971*a*). *Biopolymers* **10**, 1891.
Yathindra, N. & Rao, V. S. R. (1971*b*). *J. Polym. Sci. A2* **9**, 1149–51.
Zugenmaier, P. & Sarko, A. (1976). *Biopolymers* **15**, 2121.